

ORIGINAL ARTICLE

MUTYH, an adenine DNA glycosylase, mediates p53 tumor suppression via PARP-dependent cell death

S Oka^{1,2}, J Leon¹, D Tsuchimoto^{1,2}, K Sakumi^{1,2} and Y Nakabeppu^{1,2}

p53-regulated caspase-independent cell death has been implicated in suppression of tumorigenesis, however, the regulating mechanisms are poorly understood. We previously reported that 8-oxoguanine (8-oxoG) accumulation in nuclear DNA (nDNA) and mitochondrial DNA triggers two distinct caspase-independent cell death through buildup of single-strand DNA breaks by MutY homolog (MUTYH), an adenine DNA glycosylase. One pathway depends on poly-ADP-ribose polymerase (PARP) and the other depends on calpains. Deficiency of MUTYH causes MUTYH-associated familial adenomatous polyposis. MUTYH thereby suppresses tumorigenesis not only by avoiding mutagenesis, but also by inducing cell death. Here, we identified the functional p53-binding site in the human *MUTYH* gene and demonstrated that *MUTYH* is transcriptionally regulated by p53, especially in the p53/DNA mismatch repair enzyme, MLH1-proficient colorectal cancer-derived HCT116+Chr3 cells. MUTYH-small interfering RNA, an inhibitor for p53 or PARP suppressed cell death without an additive effect, thus revealing that MUTYH is a potential mediator of p53 tumor suppression, which is known to be upregulated by MLH1. Moreover, we found that the p53-proficient, mismatch repair protein, MLH1-proficient colorectal cancer cell line express substantial levels of MUTYH in nuclei but not in mitochondria, suggesting that 8-oxoG accumulation in nDNA triggers MLH1/PARP-dependent cell death. These results provide new insights on the molecular mechanism of tumorigenesis and potential new strategies for cancer therapies.

Oncogenesis (2014) 3, e121; doi:10.1038/oncsis.2014.35; published online 13 October 2014

INTRODUCTION

8-Oxoguanine (8-oxoG) is one of the major oxidative base lesions in DNA or nucleotides¹ and is highly mutagenic because it can pair with adenine as well as cytosine.² Studies on DNA repair mechanisms directed against 8-oxoG revealed that organisms are equipped with elaborate means of error avoidance.^{3,4} In mammals, 8-oxoG DNA glycosylase-1 (OGG1) excises 8-oxoG paired with cytosine in DNA, whereas the MutY homolog (MUTYH) removes adenine misincorporated opposite 8-oxoG in template DNA.^{4,5} These enzymes have major roles in suppressing spontaneous mutagenesis initiated by 8-oxoG. Mutant mice lacking one of these genes exhibit an increased spontaneous mutation rate and an increased susceptibility to carcinogenesis.^{6,7}

The human *MUTYH* gene is located on the short arm of chromosome 1, spans 11.2 kb and contains 16 exons. In human cells, transcription of *MUTYH* is initiated from three distinct exon 1 sequences, thus producing three types of primary transcripts, namely α , β and γ (Figure 1a). From these three primary transcripts, >15 transcripts are generated by alternative splicing at exon 1 and exon 3. Type α 3 *MUTYH* mRNA is a major *MUTYH* transcript and encodes the most abundantly expressed mitochondrial *MUTYH*.^{8–10} In contrast, *MUTYH* encoded by type β 3, β 5 or γ 3 mRNA is the most abundant nuclear isoform.

The human *MUTYH* gene has been reported as the causative gene of autosomal recessive familial adenomatous polyposis without a germline *APC* mutation and is now referred to as MUTYH-associated polyposis.^{11–13} Furthermore, *MUTYH*-null mice exhibited an increase in the spontaneous incident rate of adenoma/adenocarcinoma in the small intestine and colon, and the rate increased markedly following oxidative stress.⁶

We previously reported that accumulation of 8-oxoG in nuclear DNA (nDNA) and mitochondrial DNA (mtDNA) independently triggers two distinct cell death pathways through a common signal of buildup of single-strand DNA breaks (SSBs). During replication, adenine can be inserted opposite to 8-oxoG that is accumulated in DNA, thereby forming a considerable number of A:8-oxoG pairs in DNA. MUTYH excises adenines that are opposite to 8-oxoG through its adenine DNA glycosylase activity, and forms abasic sites that are converted to SSBs by apurinic/aprimidinic (AP) endonucleases. The buildup of SSBs in nDNA causes poly-ADP-ribose polymerase (PARP)-dependent nuclear translocation of apoptosis-inducing factor, while that in mtDNA causes mtDNA depletion and calpain activation, thereby executing caspase-independent cell death.¹⁴ MUTYH suppresses tumorigenesis not only by avoiding mutagenesis, but also by inducing cell death.⁹

Loss of p53 function has been extensively reported in many forms of cancer.^{15,16} It was reported that the transcriptional factor p53 has a crucial role in the DNA repair system by regulating transcription of the human *OGG1* gene.¹⁷ In this study, we demonstrate that the human *MUTYH* gene is a transcriptional target of p53 and thus propose that MUTYH is a potential mediator of p53 tumor suppression by inducing death of premutagenic cells generated under oxidative conditions.

RESULTS

p53 regulates expression levels of *MUTYH* mRNA and protein. To determine whether basal level expression of *MUTYH* mRNA is dependent on p53, we first compared levels of mRNAs encoding the nuclear form of *MUTYH* β , the mitochondrial form of *MUTYH* α

¹Division of Neurofunctional Genomics, Department of Immunobiology and Neuroscience, Medical Institute of Bioregulation, Kyushu University, Fukuoka, Japan and ²Research Center for Nucleotide Pool, Kyushu University, Fukuoka, Japan. Correspondence: Dr S Oka, Division of Neurofunctional Genomics, Department of Immunobiology and Neuroscience, Medical Institute of Bioregulation, Kyushu University, 3-1-1 Maidashi, Higashi-Ku, Fukuoka 812-8582, Japan. E-mail: oka@bioreg.kyushu-u.ac.jp

Received 28 April 2014; revised 15 July 2014; accepted 25 August 2014

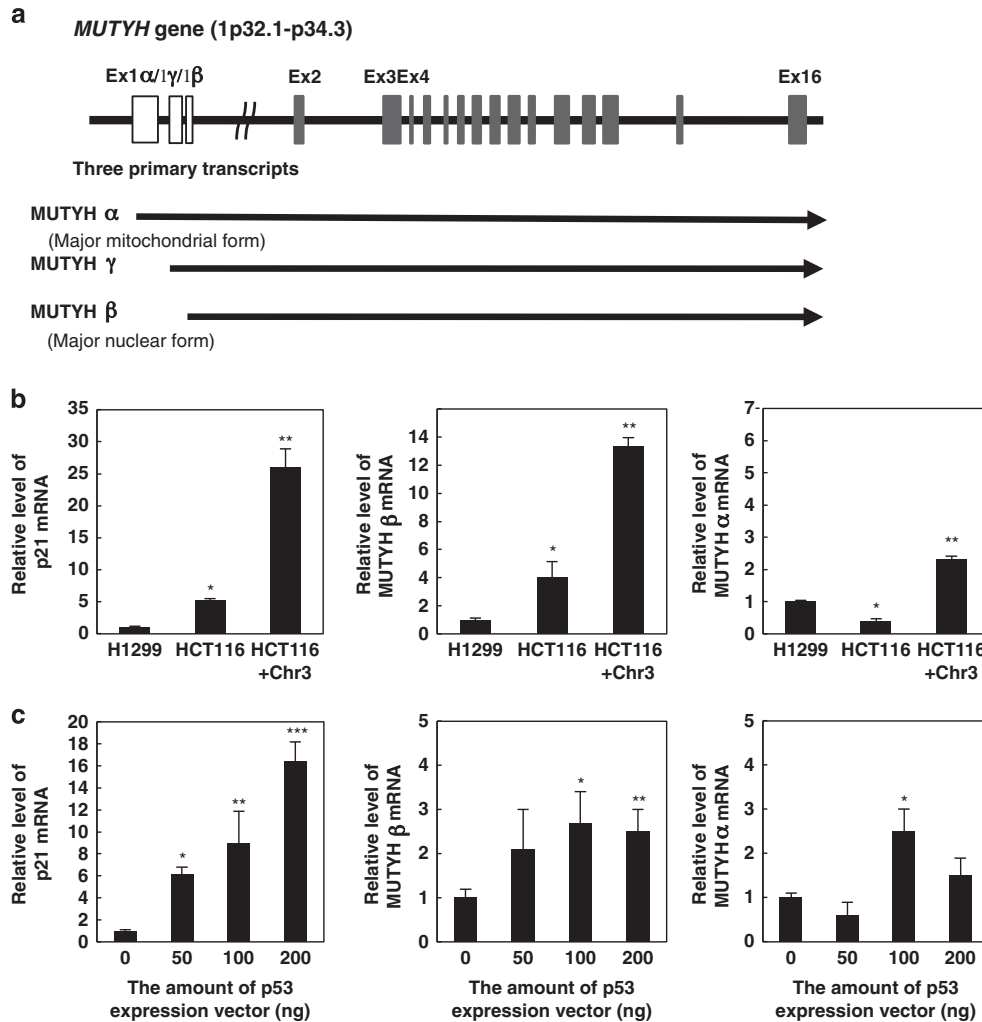


Figure 1. p53 regulates expression levels of *MUTYH* mRNA. **(a)** Genomic organization of *MUTYH*. The *MUTYH* gene produces three types of transcripts, α , β and γ . **(b)** Expression levels of *MUTYH* and p21 mRNA in p53-deficient and -proficient cells. *MUTYH* and p21 mRNA levels in HCT116 cells (p53-proficient and MLH1-deficient), HCT116+Chr3 cells (p53 and MLH1-proficient) and H1299 cells (p53-deficient and MLH1-proficient) were quantified by real-time RT-PCR. Each value was normalized for 18S ribosomal RNA level, and was shown as fold increase relative to H1299 cells. Analysis of variance (ANOVA), $P < 0.0001$. P -values with Dunnett's method are shown. * $P = 0.0369$, ** $P < 0.0001$ vs H1299 (left panel). * $P = 0.0051$, ** $P < 0.0001$ vs H1299 (middle panel). * $P = 0.0002$, ** $P < 0.0001$ vs H1299 (right panel). **(c)** Expression levels of *MUTYH* and p21 mRNA levels in H1299 cells 24 h after transfection with increasing amounts of a wild-type p53 expression plasmid. Each value was normalized for 18S ribosomal RNA level, and was shown as fold increase relative to cells without plasmid (0 ng). ANOVA, $P < 0.0434$. P -values with Dunnett's method are shown. * $P = 0.219$, ** $P = 0.0017$, *** $P < 0.0001$ vs 0 ng (left panel). * $P = 0.0468$, ** $P = 0.0277$ vs 0 ng (middle panel). * $P = 0.0016$ vs 0 ng (right panel). Results as shown in panels **(b)** and **(c)** are from three independent experiments. Mean \pm s.d.

and p21 as a target of p53 transcription in H1299, HCT116 and HCT116+Chr3 human cancer cell lines. HCT116 is a p53-proficient, DNA mismatch repair enzyme, MLH1-deficient human colorectal cancer cell line,^{18–20} and H1299 is a p53-deficient MLH1-proficient human lung small cell carcinoma cell line.²¹ Moreover, to exclude the influence of MLH1 deficiency, we used HCT116+Chr3 cells expressing functional MLH1 by transferring human chromosome 3 into HCT116 cells.²²

As shown in the left panel in Figure 1b, real-time quantitative reverse transcriptase-PCR (RT-PCR) analysis revealed that relative levels of p21 mRNA in p53-proficient HCT116 or HCT116+Chr3 cells were higher than in p53-deficient H1299 cells. As over-expression of MLH1 induces p53-Ser15 phosphorylation, which regulates transcriptional activity in HCT116 cells treated with radiomimetic chemical neocarzinostatin,²³ elevated p21 mRNA levels in HCT116+Chr3 cells is considered an MLH1-dependent increase of p53-mediated transactivation.

Levels of mRNAs encoding the nuclear and mitochondrial forms of *MUTYH* were increased in HCT116+Chr3 cells when compared with H1299 cells (Figure 1b, middle and right panel). We further examined whether the expression of *MUTYH* mRNAs was induced by the transfection of the wild-type p53 expression plasmid in p53-deficient H1299 cells. The level of p21 and *MUTYH* β mRNA was markedly increased 24 h after transfection with the p53 expression plasmid in a dose-dependent manner (Figure 1c). H1299 cells transfected with 100 ng, and to a lesser extent 200 ng, p53 expression plasmid exhibited elevated levels of the mitochondrial form of *MUTYH* α mRNA.

Next, we confirmed that expression levels of OGG1 protein were dependent on p53 by western blot analysis. The band intensity corresponding to OGG1 was low in p53-deficient H1299 cells compared with p53-proficient HCT116 cells (Figure 2a). The band intensity in HCT116 cells decreased in the presence of the chemical inhibitor of p53 pifithrin- α (PFT α). As well as OGG1,

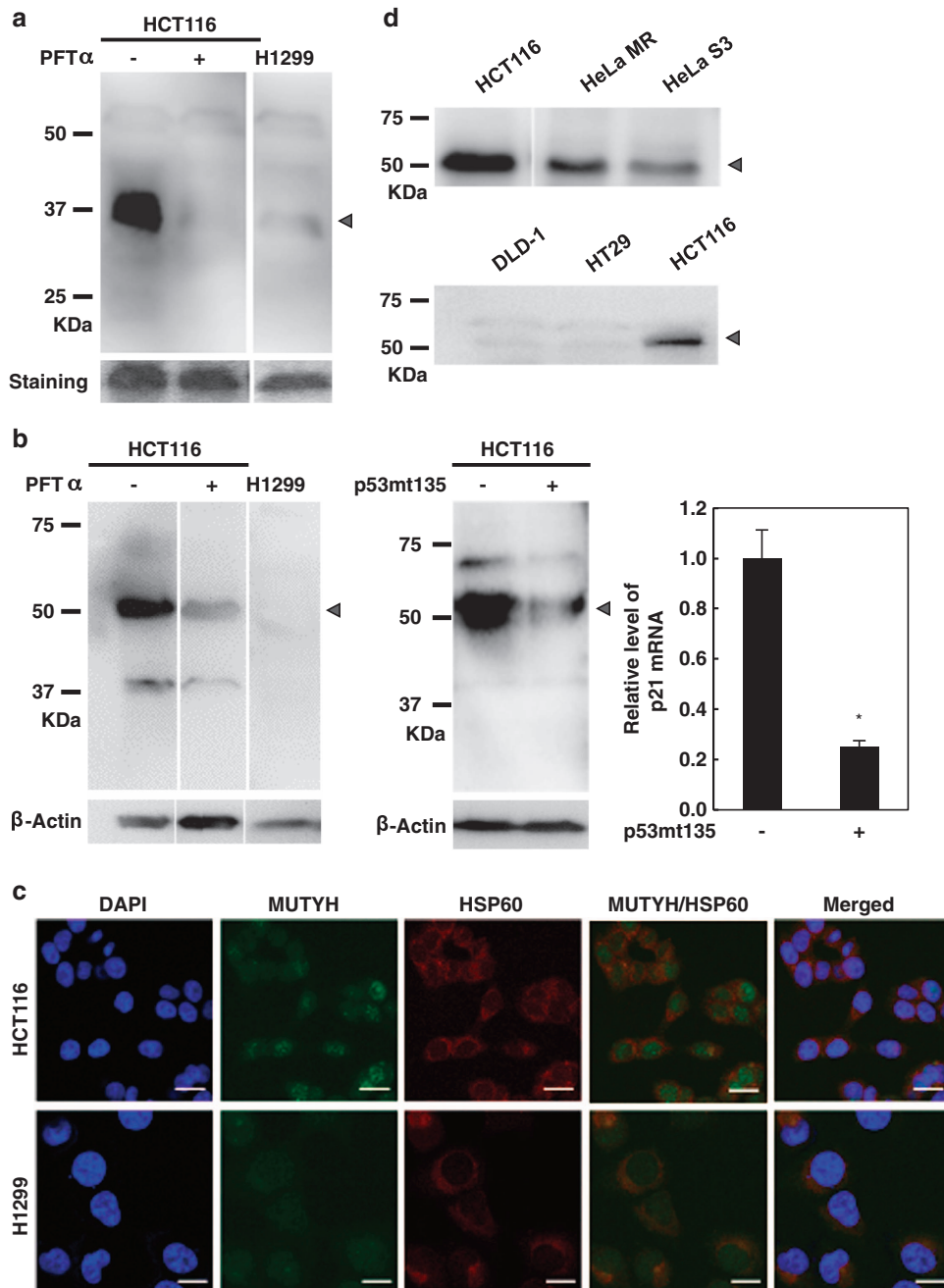


Figure 2. p53 regulates expression of MUTYH protein in various cancer cell lines. (a) Expression of OGG1 protein in H1299 cells and HCT116 cells with or without the chemical p53 inhibitor PFTα. Western blot analysis was performed using anti-HCD. Arrowhead indicates the polypeptide corresponding to OGG1. Staining, GelCode Blue Stain. (b) p53-dependent expression of MUTYH protein. Expression of MUTYH protein in H1299 cells and HCT116 cells treated with (+) or without (-) PFTα (left panel), and in HCT116 cells transfected with (+) or without (-) the dominant-negative p53 expression vector (pCMV-p53mt135) (middle panel). Western blot analysis was performed using anti-MUTYH. Arrowhead indicates the polypeptide corresponding to the nuclear isoform encoded by MUTYH β mRNA. Decreased expression of p21 mRNA in HCT116 cells transfected with pCMV-p53mt135 (right panel). * $P=0.0003$. P -value with Student's t -test is shown. Results from three independent transfection experiments are presented. Mean \pm s.d. (c) Expression and intracellular localization of MUTYH. Nuclei were stained with 4', 6-diamino-2-phenylindole (DAPI). HSP60 was used as a mitochondrial marker. Bar, 20 μ m. (d) MUTYH protein expression in human cancer cell lines with impaired p53 function (HeLa MR and HeLa S3, upper panel) and human colon cancer cell lines with p53 mutation (DLD-1 and HT29, lower panel).

the band intensity of the 53-kDa polypeptide corresponding to the nuclear isoform of MUTYH encoded by MUTYH β mRNA in p53-deficient H1299 cells was markedly lower than that in p53-proficient HCT116 cell (Figure 2b, left panel). PFTα treatment decreased the band intensity corresponding to the 53-kDa MUTYH protein β in HCT116 cells. In HCT116 cells, the 57-kDa band corresponding to the mitochondrial form of MUTYH reported in

the human T-cell lymphoblast-like Jurkat cell line was not detected.²⁴ Inactivation of p53 in HCT116 cells by transfection with a dominant-negative p53 expression vector also decreased the band intensity of the 53-kDa MUTYH protein β (Figure 2b, middle and right panels). An immunofluorescent signal for MUTYH in HCT116 cells was more intense than that in H1299 cells and was observed to mainly colocalize with 4', 6-diamino-2-phenylindole

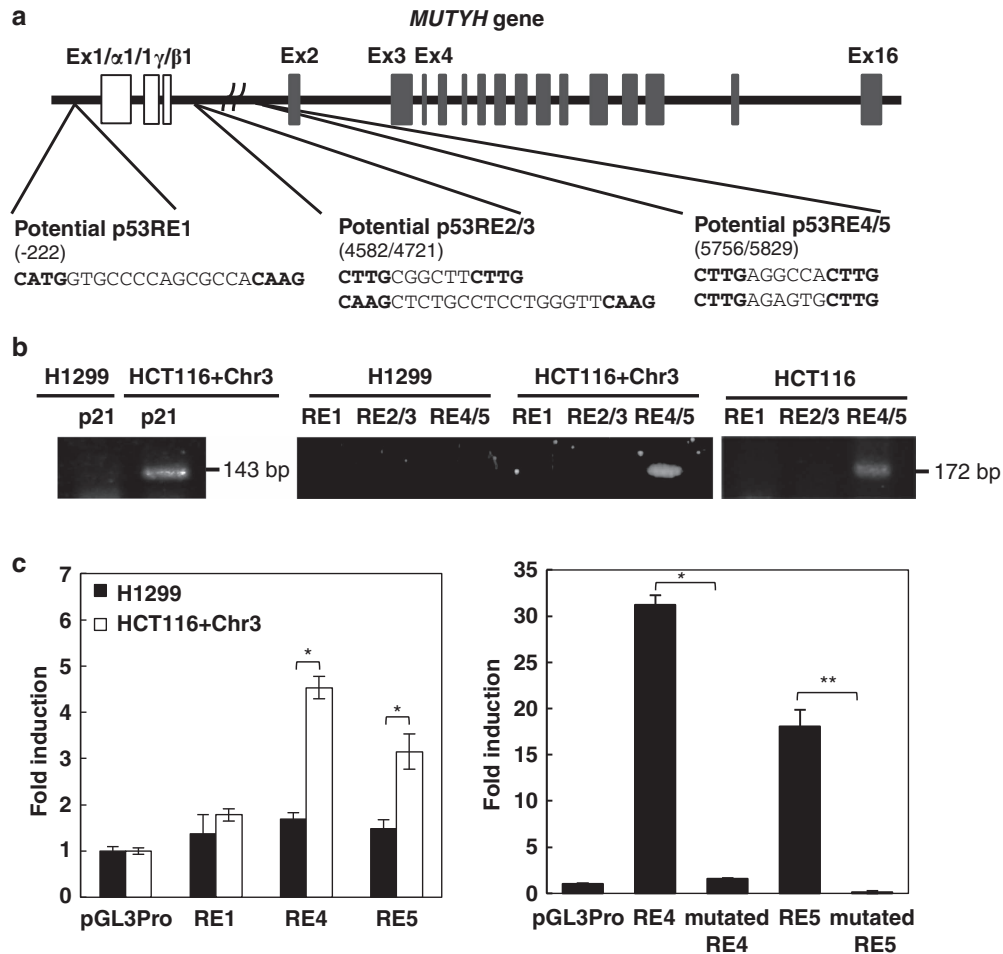


Figure 3. Identification of the functional p53REs residing in the human *MUTYH* gene. **(a)** Potential p53 response elements (p53REs) in the human *MUTYH* gene are indicated. Numbers in parentheses indicate nucleotide positions relative to the transcriptional start site of *MUTYH* α . **(b)** ChIP using the anti-p53 antibody. The precipitated DNA was analyzed by PCR using primers specific for p21 as a positive control for p53 binding or primers specific for each p53REs. Results from one of two independent experiments are presented. **(c)** Luciferase reporter assay. H1299 and HCT116+Chr3 cells were co-transfected with 100 ng of pGL3-promoter vector containing each p53REs and 10 ng of phRL-SV40 vector (left panel). Luciferase activities are shown to represent the fold induction relative to the activity in cells transfected with the pGL3-promoter luciferase empty vector (pGL3pro), as shown on the left side of each panel. HCT116+Chr3 cells were co-transfected with 200 ng of pGL3-promoter vector containing either p53RE or mutated p53RE (mutation in p53-binding motif, CTTG \rightarrow AGGT) and 20 ng of phRL-SV40 vector (right panel). * $P=0.0495$ (left panel). * $P=0.0495$, ** $P=0.0463$ (right panel). P -values with Wilcoxon test are shown. Results from three independent transfection experiments are presented. Mean \pm s.d.

staining, a nuclear marker, but not the mitochondrial protein HSP60 (Figure 2c). These results suggest that expression levels of the nuclear isoform of *MUTYH* encoded by *MUTYH* β mRNA, are positively regulated by p53 in the human colorectal cancer cell line.

Expression levels of *MUTYH* protein in human cancer cell lines with varying p53 statuses

We next examined *MUTYH* protein expression levels in human cancer cell lines with varying p53 statuses. HeLa MR and HeLa53 cells, which are human epithelioid cervical carcinoma cell lines, have impaired p53 function because of the expression of the human papilloma virus E6 gene product.²⁵ In HeLa cells, protein expression of the 53-kDa nuclear isoform of *MUTYH* was lower than that in p53-proficient HCT116 cells (Figure 2d, upper panel). Moreover, in the human colon cancer cell lines with p53 mutations, DLD-1 cells with S241F and HT29 cells with R273H,²⁶ exhibited a clear reduction in expression levels when compared with HCT116 cells (Figure 2d, lower panel).

p53 responsive elements reside within the human *MUTYH* gene

To identify potential p53 responsive elements (p53REs), we searched the genomic sequence of the human *MUTYH* gene and sequences 1.5 kb upstream using the consensus DNA sequence element for p53 binding, RRRCWWGYYY as a tandem repeat or YCTYCWAGR, and detected the five potential p53 response elements, p53RE1 in the 5' upstream region of the *MUTYH* gene, RE2/3 and RE4/5 in intron 1 (Figure 3a).²⁷ As p53 is required to directly bind to p53REs to activate the transcription of its target, we next performed chromatin immunoprecipitation (ChIP) analysis using p53-deficient, MLH1-proficient H1299, p53-proficient, MLH1-proficient HCT116+Chr3 or p53-proficient, MLH1-deficient HCT116 cells (Figure 3b). The co-precipitated DNA with p53 was subjected to genomic PCR using primers specific for p53RE in p21 as a positive control for p53 binding or primers specific to each of the potential p53REs. As a result, RE4/5 was found to be associated with p53 in HCT116+Chr3 or HCT116 cells, implicating these sites as the p53 response element. Next, to confirm whether these sites were the functional responsive element, we constructed pGL3-promoter luciferase reporters containing p53RE1, p53RE4 or p53RE5. The luciferase activity in cells transfected with the

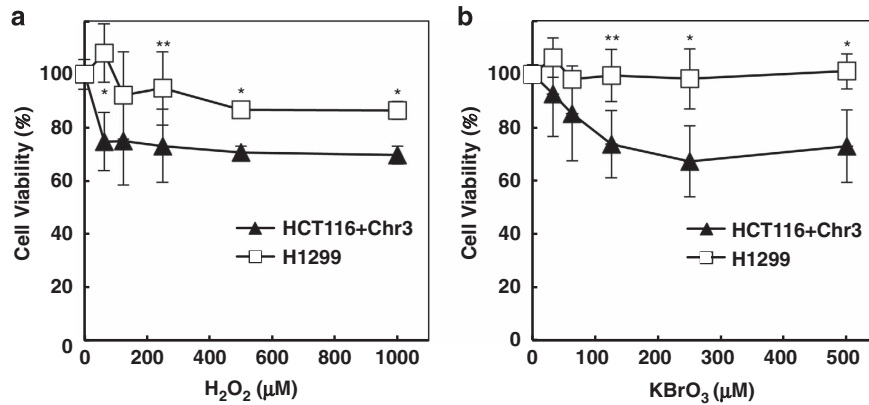


Figure 4. p53-proficient HCT116+Chr3 cells are more sensitive to either KBrO₃ or H₂O₂. **(a, b)** Cell viability under oxidative stress conditions. Cells were incubated in medium containing various concentrations of H₂O₂ **(a)** or KBrO₃ **(b)** for 24 h. **P* = 0.0209, ***P* = 0.0433. *P*-values with Wilcoxon test are shown. Results from more than four independent experiments are presented. Mean ± s.d.

pGL3-promoter luciferase reporter without p53RE was used as a control. As shown in Figure 3c (left panel), the luciferase activity in H1299 cells was not increased by transfection of the reporter containing each p53REs. In contrast, the luciferase activity in HCT116+Chr3 cells transfected with the vector containing p53RE4 or p53RE5 was markedly increased when compared with the control (Figure 3c, left panel). This transcriptional activation of luciferase was impaired by mutations of p53RE4 or p53RE5 (Figure 3c, right panel). These results indicate that RE4 and RE5 are the functional p53RE in the *MUTYH* genome.

The role of *MUTYH* as a downstream target of p53 in the oxidative stress-induced cell death pathway

Next, we examined the influence of p53 deficiency on the sensitivity to oxidative stress in the human cancer cell lines. The mismatch repair enzyme, MLH1, has been reported to be involved in oxidative stress-induced cell death by inhibiting RNA polymerase II-dependent transcription on damaged DNA templates.²⁸ To exclude the influence of MLH1 deficiency on cell death, we compared the p53-proficient, MLH1-proficient HCT116+Chr3 cells and p53-deficient, MLH1-proficient H1299 cells. Cells were incubated in medium containing various concentrations of hydrogen peroxide (H₂O₂) or potassium bromate (KBrO₃), a strong inducer of oxidative stress,²⁹ for 24 h. As a result, p53-proficient HCT116+Chr3 cells were more sensitive to both H₂O₂ and KBrO₃ than p53-deficient H1299 cells (Figures 4a and b).

To examine whether *MUTYH* was a downstream mediator of p53 in cell death, we compared cell viability following suppression of *MUTYH*, p53 or both (Figure 5). We first examined the effects of two different *MUTYH*-small interfering RNAs (siRNAs) (YsiRNA-2 and YsiRNA-3) separately or together on H₂O₂-induced cell death in HCT116+Chr3 cells. The cells transfected with either siRNA separately or both siRNAs together acquired significant resistance to cell death induced by H₂O₂ (Figure 5a, left panel). The transfection procedure did not affect the cell viability after exposure to H₂O₂, as shown by the glyceraldehyde 3-phosphate dehydrogenase-negative siRNA. The levels of *MUTYH* mRNA were effectively reduced 24 h after the transfection (Figure 5a, right panel). Next, HCT116+Chr3 cells were pretreated for 24 h with PFTα, a specific p53 inhibitor, and then incubated with PFTα for 24 h in the presence or absence of the two *MUTYH*-siRNAs. Cells were then exposed to different concentrations of H₂O₂ for 24 h. Cells only exposed to H₂O₂ without any pretreatment were used as a control. As shown in Figure 5b, although suppression of *MUTYH* or p53 alone increased resistance to H₂O₂, transfection of both *MUTYH*-siRNAs showed no additive effect on viability following p53 inhibition. We thus conclude that *MUTYH* is a

potential mediator of p53 in the oxidative stress-induced cell death pathway. We previously reported that accumulation of 8-oxoG in nuclear and mtDNA independently triggers two distinct cell death pathways: one depends on PARP and the other depends on calpain. Both pathways induce the buildup of SSBs through *MUTYH*-initiated base excision repair.¹⁴ To clarify which type of cell death pathway is concerned with the process mediated by *MUTYH*, we next examined cell viability in the presence of the calpain inhibitor MDL28170 or PARP inhibitor 3-aminobenzamide (3-AB) in HCT116+Chr3 cells. As a result, cell viability was not improved by MDL28170, whereas 3-AB efficiently increased viability (Figure 5c). We further examined whether PARP inhibition influences sensitivity to oxidative stress following p53 inhibition in HCT116+Chr3 cells (Figure 5d). As a result, 3-AB had no additive effect on the viability of cells pretreated with PFTα. These results suggest that PARP, but not calpains, has a role in p53-mediated H₂O₂-induced cell death. Finally, the general pan caspase inhibitor Z-VAD-fmk did not alter the sensitivity to H₂O₂, indicating that caspases are not involved in oxidative stress-induced cell death in HCT116+Chr3 cells (Figure 5e).

The status of p53 or DNA mismatch repair affects *MUTYH*-dependent cell death

Finally, we examined whether the effect of *MUTYH*-siRNA on H₂O₂-induced cell death depends on the status of p53 or DNA mismatch repair. As shown in Figures 6a and b, *MUTYH* knockdown increased cell viability in p53-proficient HCT116+Chr3, but not in p53-deficient H1299 cells, consistent with the finding in Figure 5b. Moreover, *MUTYH* knockdown increased the viability in MLH1-proficient HCT116+Chr3 cells, but not in MLH1-deficient HCT116 cells (Figures 6b and c). Similar to other p53-deficient cell lines, *MUTYH* knockdown had no effect on the sensitivity to H₂O₂ in p53-deficient, MSH6-deficient DLD-1 cells (Figure 6d). As shown in Figure 6e, MLH1 knockdown in HCT116+Chr3 cells largely abolished the H₂O₂ resistance acquired by *MUTYH* knockdown. We next confirmed whether *MUTYH* knockdown suppressed H₂O₂-induced cell death in HCT116+Chr3 cells. As shown in Figure 6f, the percentage of dead cells (12.8%) in control cell cultures after exposure to 200 μM H₂O₂ had decreased to 3.5% in the presence of *MUTYH*-siRNAs. These results indicate that both wild-type p53 and MLH1 are required for the induction of *MUTYH*-dependent cell death under oxidative stress conditions.

DISCUSSION

Our major conclusions in this study are that human *MUTYH* is transcriptionally regulated by p53, and that *MUTYH* is a potential

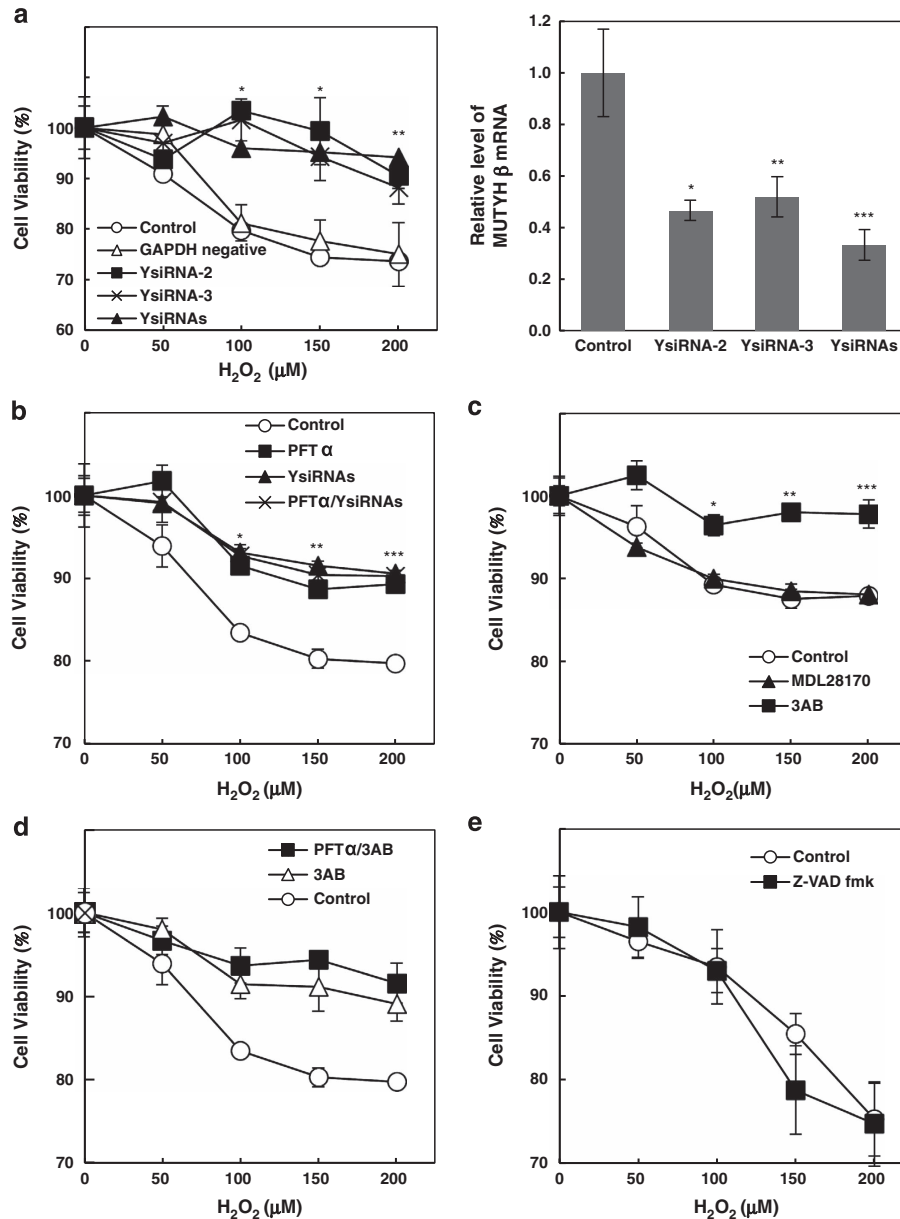


Figure 5. MUTYH is a downstream mediator of p53-induced cell death under oxidative stress conditions. **(a)** The effects of MUTYH-siRNAs on H_2O_2 -induced cell death in HCT116+Chr3 cells. HCT116+Chr3 cells were transfected with YsiRNA-2 and YsiRNA-3 separately or together (YsiRNAs) 24 h before H_2O_2 challenge. Control cells were exposed to H_2O_2 without transfection. * $P < 0.005$ (control vs YsiRNA-2, -3, YsiRNAs), ** $P < 0.005$ (control vs YsiRNA-2, YsiRNAs). P -values with Tukey's HSD test are shown. Results from more than four independent transfection experiments are presented. Mean \pm s.e.m. Expression levels of MUTYH mRNA in HCT116+Chr3 cells 24 h after siRNA transfection (right panel). * $P = 0.0043$, ** $P = 0.0037$, *** $P = 0.0013$ vs Control. P -values with Dunnett's method are shown. Results from three independent transfection experiments are presented. Mean \pm s.d. **(b)** Suppression of cell death by a p53 inhibitor and MUTYH-siRNAs. HCT116+Chr3 cells were cultured in medium with or without 20 nM PFT α for 24 h and then transfected with the two MUTYH-siRNAs (YsiRNAs) in the presence or absence of PFT α . Twenty-four hours after transfection, cells were incubated in medium containing various concentrations of H_2O_2 for 24 h. Cells only exposed to H_2O_2 without any pretreatment were used as a control. Control (* $P = 0.022$, ** $P = 0.013$, *** $P = 0.0006$) vs PFT α . P -values with Tukey's HSD test are shown. **(c)** Suppression of cell death by an inhibitor for PARP but not for calpains. HCT116+Chr3 cells were pre-incubated with 20 μ M MDL28170 or 10 mM 3-AB for 60 min and then exposed to H_2O_2 for 24 h. Control cells were exposed to H_2O_2 without any pretreatment. Control (* $P = 0.0007$, ** $P = 0.0001$, *** $P = 0.0004$) vs 3-AB. P -values with Tukey's HSD test are shown. **(d)** Effect of 3-AB on H_2O_2 -induced cell death following PFT α pretreatment. HCT116+Chr3 cells were cultured in medium with or without 20 nM PFT α for 24 h and incubated with 10 mM 3-AB for 60 min and then exposed to H_2O_2 for 24 h. **(e)** Caspase inhibitor does not suppress H_2O_2 -induced cell death. HCT116+Chr3 cells were pre-incubated with 50 μ M Z-VAD-fmk for 60 min and then exposed to H_2O_2 for 24 h. Results shown in panel **(b-e)** are from more than four independent experiments. Mean \pm s.e.m.

mediator of p53 tumor suppression by inducing death of premutagenic cells generated under oxidative conditions. Moreover, we propose that PARP is involved in p53-mediated oxidative stress-induced cell death.

Transcriptional regulation of *MUTYH* gene expression by p53
In response to a variety of types of DNA damage, p53 regulates a number of downstream cellular processes such as cell cycle arrest, apoptosis and DNA repair. In the DNA repair machinery, p53 can

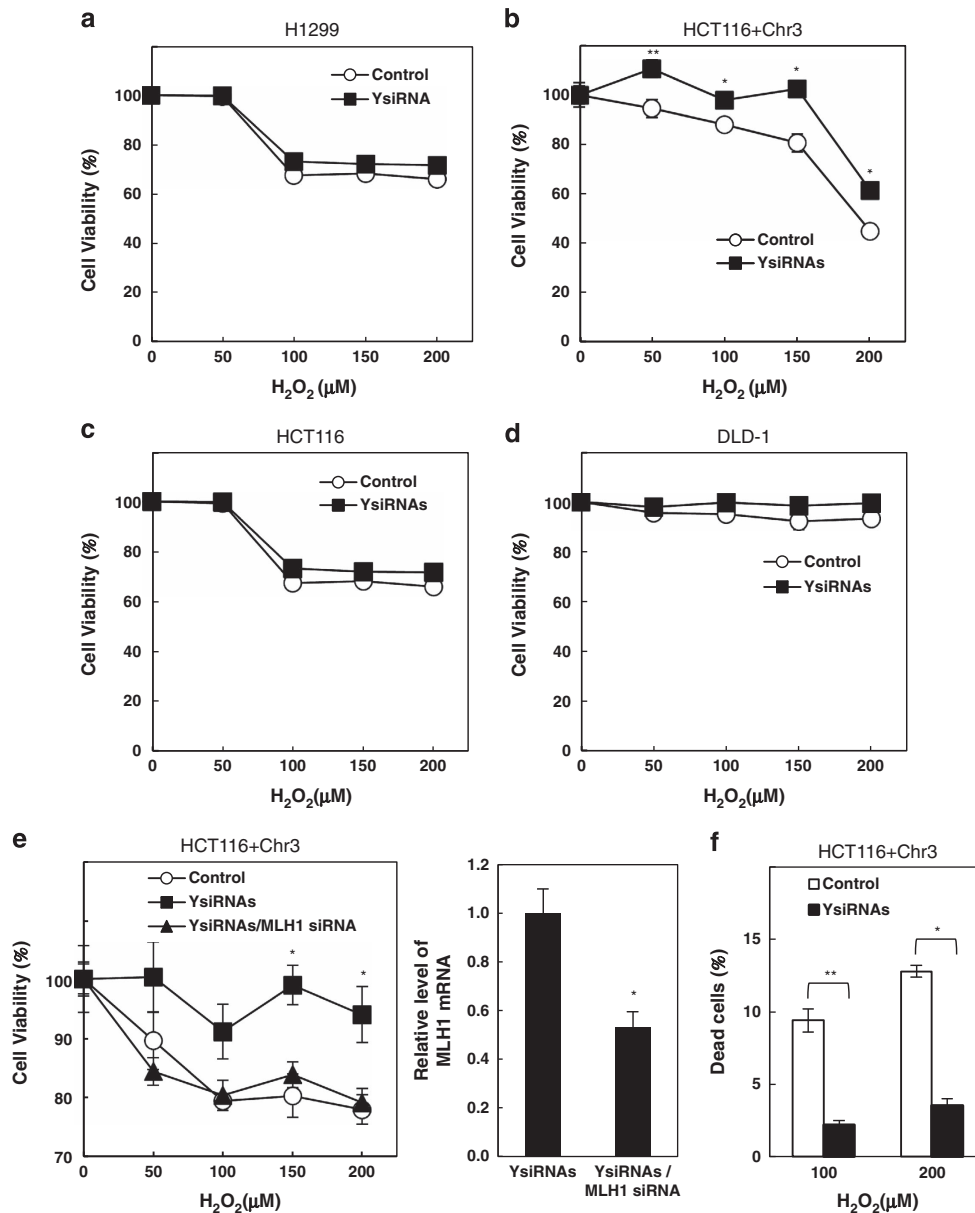


Figure 6. The status of p53 or DNA mismatch repair enzyme affects MUTYH-dependent cell death in cancer cell lines. The effect of MUTYH-siRNA on H₂O₂-induced cell death in H1299 (a), HCT116+Chr3 (b), HCT116 (c) and DLD-1 cells (d). Control cells were exposed to H₂O₂ without transfection. **P* = 0.0209, ***P* = 0.0433. *P*-values with Wilcoxon test are shown. Results from more than four independent experiments are presented. Mean ± s.e.m. (e) MLH1 knockdown in HCT116+Chr3 cells abolished the H₂O₂ resistance acquired by MUTYH knockdown (left panel). HCT116+Chr3 cells were transfected with MUTYH siRNA-2 and 3 (YsiRNAs) or together with MLH1 siRNA (YsiRNAs/MLH1 siRNA). Twenty-four hours after transfection, cells were incubated in medium containing various concentrations of H₂O₂ for 24 h. Cells only exposed to H₂O₂ without any pretreatment were used as a control. **P* = 0.0209 (YsiRNAs vs YsiRNAs/MLH1 siRNA). *P*-values with Tukey's HSD test are shown. Results from four independent experiments are presented. Mean ± s.e.m. Expression levels of MLH1 mRNA in HCT116+Chr3 cells transfected with YsiRNAs or YsiRNAs/MLH1 siRNA (right panel). **P* = 0.0013. *P*-value with Student's *t*-test is shown. Results from three independent transfection experiments are presented. Mean ± s.d. (f) Suppression of H₂O₂-induced cell death by MUTYH-siRNAs. HCT116+Chr3 cells were transfected with MUTYH-siRNA-2 and 3 (YsiRNAs), cultured for 24 h and exposed to H₂O₂. Percentages of dead cells were determined 24 h after the exposure. Control cells were exposed to H₂O₂ without any pretreatment. Control (**P* = 0.0304, ***P* = 0.0294) vs YsiRNA. *P*-values with Student's *t*-test are shown Mean ± s.e.m.

act at several levels that include interaction with APE1 (an AP endonuclease), DNA polymerase β, enhancement of incision of the damaged base and possibly transcriptional regulation of *OGG1* to excise 8-oxoG paired with cytosine in DNA.^{17,30} Moreover, it has been shown that human *MUTYH* is transcriptionally regulated by the p53 family member p73 through a potential binding site (5'-GCATGGGGCTGATGGAGCATG-3') located at -33 from the transcriptional start site of *MUTYH* α mRNA.³¹ In this study, we

identified two functional p53REs residing within the first intron of the human *MUTYH* gene. The p53RE4 (5'-CTTGAGGCCACTTG-3') and p53RE5 (5'-CTTGAGAGTGCTTG-3') located at 5756 and 5829, respectively (Figure 3a). Real-time RT-PCR analysis revealed that the levels of *MUTYH* mRNA were markedly increased following transfection with the wild-type p53 expression plasmid. Our findings indicate that *MUTYH* is a target of transcriptional regulation by p53. Transcription factor p53 precisely regulates

the OGG1-initiated base excision repair pathway through several steps. Moreover, the mitochondrial form of MUTYH protein was not detected by western blot analysis in p53-proficient HCT116 cells, suggesting that the expression of the mitochondrial form of MUTYH is regulated by a p53-independent mechanism.

PARP, but not calpains, has a role in oxidative stress-induced p53-mediated cell death

In this study, we found that the PARP inhibitor, but not the calpain inhibitor, suppresses H₂O₂-induced cell death in p53-proficient human colorectal cancer cells. PARP is a molecular nick sensor that binds specifically to SSBs, and its specific activity involves catalyzing poly-ADP ribosylation of cellular proteins or of PARP itself and increasing its enzymatic activity by approximately 500-fold.³² In addition, apoptosis-inducing factor translocates to the nucleus in a PARP-dependent manner, and apoptosis-inducing factor/EndoG-mediated nDNA fragmentation represents a major mechanism of caspase-independent apoptosis.^{33,34} Our data suggest that the PARP-dependent cell death pathway induced by 8-oxoG accumulation in nDNA is mainly activated in the p53-proficient colon cancer cell line under oxidative stress conditions. As shown in Figures 5b and 6b, MUTYH knockdown rescued 10–20% of cells, and this could be equivalent to the population of S-phase cells that can generate SSBs through base excision repair initiated by the nuclear form of MUTYH. In contrast, the calpain inhibitor did not suppress cell death and the mitochondrial form of the MUTYH protein was not detected, suggesting that defects in the cell death pathway induced by 8-oxoG accumulation in mtDNA contribute to decreased sensitivity to oxidative stress, resulting in tumorigenesis or survival of cancer cells (Figure 7).

In Figure 6, we found that the effect of MUTYH-siRNA on H₂O₂-induced cell death depends on wild-type p53 and MLH1. The MSH2/MSH6 complex has been reported to be physically associated with MUTYH at the MSH6-binding site and the interaction stimulates MUTYH activity.^{35,36} Kanagaraj *et al.* recently

showed that depletion of MUTYH suppresses the hypersensitivity of cells lacking the Werner syndrome helicase/exonuclease and/or pol λ to H₂O₂.³⁷ These studies, and our results, provide evidence that the status of p53 and DNA repair proteins is involved in the induction of MUTYH-dependent cell death under oxidative stress conditions.

In addition to MLH1, HCT116 cells are defective in the mismatch repair enzyme MSH3.³⁸ As the HCT116+Chr3 cell line has been complemented with an additional chromosome 3 to restore *MLH1* gene function, this cell line is still MSH3 deficient. However, a recent study has reported that MSH3 translocates from the nuclei to the cytoplasm under oxidative stress conditions, resulting in a loss-of-function.³⁹ Therefore, it is most likely that H1299 cell also exhibit MSH3 dysfunction after H₂O₂ treatment as do HCT116+Chr3 cells.

MUTYH as a potential mediator of p53 tumor suppression

Several studies indicate that most human cancers show loss of normal p53 function.⁴⁰ In response to various stressors, p53 can induce cell death via a caspase-dependent and -independent pathway, with the cell death being implicated in suppression of tumorigenesis.^{41,42} Recently, it was reported that LL-37, the human cathelicidin, activates a caspase-independent apoptotic cascade regulated by p53 that contributes to the suppression of colon cancer.⁴² LL-37 activates a GPCR-p53-Bax/Bak/Bcl-2 signaling pathway that triggers apoptosis-inducing factor/EndoG-mediated apoptosis. We previously demonstrated that accumulation of 8-oxoG in nDNA and mtDNA independently triggers two distinct caspase-independent cell death pathways through MUTYH-initiated base excision repair.¹⁴ Thus, p53 deficiency leads to MUTYH dysfunction in stem or progenitor cells, which results in escape from programmed cell death under oxidative stress. Accumulated 8-oxoG causes various mutations in tumor-suppressor genes or proto-oncogenes such as *APC* or *KRAS*, thereby promoting tumorigenesis (Figure 7).

The p53-mediated cell death pathway is also known to be involved in the development of neurodegenerative diseases.⁴³ Increased p53 immunoreactivity was observed in sporadic Alzheimer's disease, especially in sub-populations of cortical neurons undergoing neurofibrillary degeneration.⁴⁴ The amyloid β -42 peptide, which has a pivotal role in Alzheimer's disease, binds to the p53 promoter and enhances transcription, resulting in apoptosis of primary human neurons.⁴⁵ Oxidative stress is considered to be important in the etiology of several neurodegenerative disorders.⁴⁶ We recently reported that 8-oxoG accumulation in nDNA or mtDNA causes neurodegeneration during MUTYH-mediated DNA base excision repair.⁴⁷ Moreover, increased MUTYH expression was observed in the mitochondria of substantia nigra neurons in Parkinson's disease patients.⁴⁸ These findings suggest that enhancement of *MUTYH* expression by p53 can lead to neuronal loss under oxidative stress conditions.

In conclusion, we propose that MUTYH can be an effective mediator for anticancer therapies. Radiation or anticancer drugs are known to produce ROS resulting in increased accumulation of 8-oxoG in cellular DNA, thereby MUTYH-dependent cell death could effectively eliminate cancer cells. To minimize the side effects of anticancer therapies, MUTYH inhibitors selectively delivered to normal tissue would be beneficial. Thus, we emphasize that the identification of p53 status and DNA repair proteins including MUTYH is important for the accurate assessment and treatment of cancer.

MATERIALS AND METHODS

Cell lines

The H1299 non-small cell lung carcinoma cell line²¹ and HeLa MR and HeLaS3²⁵ human cervical carcinoma cell lines were laboratory stocks. The

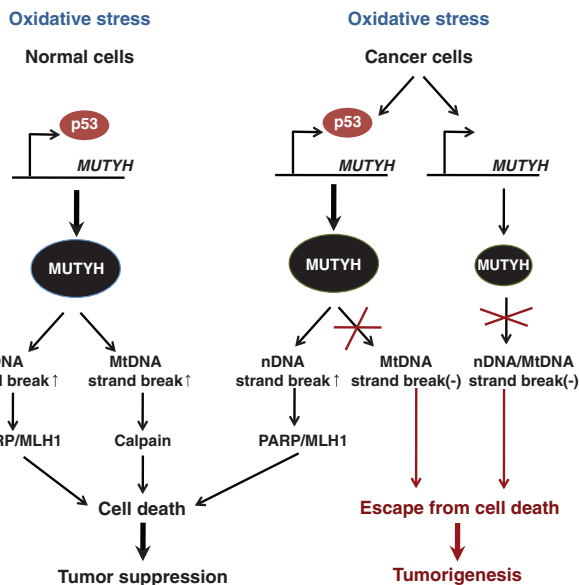


Figure 7. MUTYH mediates p53 tumor suppression via PARP/MLH1-dependent cell death. p53 deficiency leads to MUTYH dysfunction in stem or progenitor cells, which results in escape from programmed cell death under oxidative stress. Accumulated 8-oxoG causes various mutations in tumor-suppressor genes or proto-oncogenes, thereby promoting tumorigenesis. Loss of the mitochondrial form of MUTYH in p53-proficient cells also induces carcinogenesis via escape from cell death.

HCT116 colon adenocarcinoma cell line was purchased from ATCC (Manassas, VA, USA). The human colon cancer cell lines, DLD-1 and HT29,²⁶ were a gift from Dr S Oda (National Kyushu Cancer Center, Fukuoka, Japan). The HCT116+Chr3 cell line²² was a gift from Dr CR Boland (Baylor University Medical Center, Dallas, TX, USA). Cells were cultured in Dulbecco's modified Eagle's medium (Invitrogen, Carlsbad, CA, USA) supplemented with 10% (v/v) heat-inactivated fetal bovine serum, 100 µg/ml streptomycin and 100 units/ml penicillin, at 37 °C in 5% (v/v) CO₂.

Real-time quantitative RT-PCR analysis

Total RNA was extracted using ISOGEN (Nippon Gene, Tokyo, Japan). Two micrograms each of RNA sample was reverse-transcribed using the High Capacity cDNA Reverse Transcription Kit (Applied Biosystems, Foster City, CA, USA) and random hexamer primers. Real-time quantitative RT-PCR was performed on an ABI 7500 machine (Applied Biosystems). Each reaction was performed with the appropriate amount of complementary DNA, optimized amount of forward and reverse primers and 12.5 µl 2 × Power SYBR Green Master Mix (Applied Biosystems) in a total volume of 25 µl. The primers used for PCR were as follows: MUTYH α-specific primers (forward, 5'-GAGGAGCCTCTAGAACTATGA-3'; reverse, 5'-CTTGGCCTGACTGTTGTCT-3'), MUTYH β-specific primers (forward, 5'-CTCCGTGTTCTGCTGCTTC-3'; reverse, 5'-CTTGGCCTGACTGTTGTCT-3'), p21-specific primers (forward, 5'-TGGAGACTCTCAGGTCGAAA-3'; reverse, 5'-GGCGTTGGAGTGGTAGAAATC-3'), 18S ribosomal RNA-specific primers (forward, 5'-CTTAGAGGGACAAGTGCGC-3'; reverse, 5'-GGACATCTAAGGCATCACA-3') and MLH1-specific primers (forward, 5'-TGGGACGAAGAAAAGGAATG-3'; reverse, 5'-TCCAGGAGTTTGAATGGAG-3').

Plasmids, transfection and luciferase reporter assay

The pCMV-p53 vector that encodes wild-type p53 and the pCMV-p53mt135 vector that encodes dominant-negative p53 (C135Y)⁴⁹ were purchased from Clontech Laboratories Inc. (Mountain View, CA, USA). Cells were transfected with the pCMV-p53 vector using Effectene (Qiagen, Germantown, MD, USA) and subjected to real-time quantitative RT-PCR 24 h after transfection. To inactivate endogenous p53 in HCT116 cells, cells were transfected with the pCMV-p53mt135 vector using Effectene and selected with 400 ng/µl G418 (Invitrogen) for 72 h after transfection. After 24-h culture, cells were subjected to real-time quantitative RT-PCR and western blot analysis.

Plasmids for the luciferase reporter assay were created using the pGL3-promoter vector (Promega, Madison, WI, USA). Synthetic oligonucleotides containing p53RE or mutated p53RE (mutation in p53-binding motif, CTTG → AGGT) were cloned to the *SacI* and *XmaI* sites of the pGL3-promoter vector. All clones were sequenced to rule out any mutations. For luciferase assay, cells were cultured in 24-well plates and each well was co-transfected with the pGL3-promoter vector containing the p53RE and pRL-SV40 plasmid encoding Renilla luciferase (Promega). The luciferase activity was measured using the Dual-Gro Luciferase Reporter Assay system (Promega) 48 h after transfection. The transfection efficiency was determined by the Renilla luciferase activity.

Western blot analysis and Immunostaining

Anti-HCD against the highly conserved domain of hOGG1 isoforms has been described.⁵⁰ Anti-MUTYH rabbit polyclonal antibodies were used as described previously.²⁴ Antibodies against PCNA (PC10; Abcam, Cambridge, MA, USA), HSP60 (LK-1; StressGen, San Diego, CA, USA) were also used. For immunostaining, digital images were separately captured from identical fields using an LSM-510 Meta confocal microscopy system (Carl Zeiss, Jena, Germany). Images were processed for publication by Adobe Photoshop CS5 software (Adobe System Inc., San Jose, CA, USA).

Chromatin immunoprecipitation

ChIP assays were performed using the EZ ChIP (Millipore, Billerica, MA, USA) according to the manufacturer's protocol with some modifications. Briefly, 4 × 10⁶ cells per immunoprecipitation were cross-linked with 37% (v/v) formaldehyde and sonicated to produce chromatin fragments between 500 and 1000 bp. Chromatin was subsequently incubated with anti-p53 antibody (Ab-1; Oncogene Science, Cambridge, MA, USA) overnight at 4 °C. Immunoprecipitated samples were treated as described by the manufacturer's instructions, and purified DNA from the ChIP samples was assayed by PCR. The primers used for PCR were as follows: p21 (forward, 5'-CATCCCCACAGCAGAGGAGAA-3'; reverse, 5'-ACCCAGGC

TTGGAGCAGCTA-3'), p53RE1 (forward, 5'-TGTAGGGCTGAGGATCTCA-3'; reverse, 5'-GAAGGTAGGACGTATTGGGA-3'), p53RE2/3 (forward, 5'-GGG GTGGAAGGATCAGAGAG-3'; reverse, 5'-CCAAAAAATTAGCCAGACG-3') and p53RE4/5 (forward, 5'-TCTTTGCATGTCTCCAGGCC-3'; reverse, 5'-CCC TCTCATCCACCATTAC-3').

Cell viability and cell death assay

Cell viability was determined using the 2-(2-methoxy-4-nitrophenyl)-3-(4-nitrophenyl)-5-(2,4-disulfophenyl)-2H-tetrazolium, monosodium salt (WST-8) assay and the Cell Counting Kit-8 (Wako Pure Chemical Industries, Osaka, Japan). In brief, cells were cultured in 96-well plates to ~70% confluence using MEM (Invitrogen) supplemented with 10% (v/v) heat-inactivated fetal bovine serum, 100 µg/ml streptomycin and 100 units/ml penicillin and incubated with medium containing various concentrations of H₂O₂ or KBrO₃, followed by incubation with WST-8. Absorbance of WST-8 formazan dye at 450 nm was measured, and relative cell viability was determined as a percentage of the absorbance of cells without exposure. MDL28170 from BIOMOL (Phymouth Meeting, PA, USA); PFTα, 3-AB was obtained from Sigma-Aldrich (St Louis, MO, USA). To determine the percentage of dead cells, the number of dead cells stained with both Hoechst33342 and propidium iodide was divided by the total number of cells stained with Hoechst.

siRNA and transfections

Two human MUTYH-siRNAs (YsiRNA-2, s9091; YsiRNA-3, s9092) and glyceraldehyde 3-phosphate dehydrogenase-negative siRNA (4603G) as a negative control were purchased from Ambion (Austin, TX, USA). Human MLH1 siRNA (Silencer MLH1 siRNA; 119549) was purchased from Applied Biosystems. Cells were transfected with each siRNA using a siPORT lipid, Silencer TM siRNA Transfection Kit (Ambion).

Statistical analysis

All statistical analyses were carried out using JMP 8.01 software (SAS Institute, Cary, NC, USA).

ABBREVIATIONS

3-AB, 3-aminobenzamide; 8-oxoG, 8-oxoguanine; ChIP, chromatin immunoprecipitation; H₂O₂, hydrogen peroxide; KBrO₃, potassium bromate; mtDNA, mitochondrial DNA; MUTYH, MutY homolog; nDNA, nuclear DNA; OGG1, 8-oxoG DNA glycosylase-1; PARP, poly-ADP-ribose polymerase; PFTα, pifithrin-α; p53REs, p53 responsive elements; SSBs, single-strand DNA breaks

CONFLICT OF INTEREST

The authors declare no conflict of interest.

ACKNOWLEDGEMENTS

We thank Dr C Richard Boland (Baylor University Medical Center, Dallas, TX, USA) and Dr H Kitao (Department of Molecular Oncology, Graduate School of Medical Sciences, Kyushu University, Fukuoka, Japan) for the generous gift of HCT116+Chr3, and Dr S Oda (National Kyushu Cancer Center, Fukuoka, Japan) for the generous gift of DLD-1 and HT29 cell lines. Dr Dongchon Kang (Department of Clinical Chemistry and Laboratory Medicine, Graduate School of Medical Sciences, Kyushu University, Fukuoka, Japan) for providing us with the opportunity to conduct this study. We also thank K Asakawa and T Kuwano for their technical assistance. This work was supported by JSPS KAKENHI grant numbers 22501014 (to SO) and 22221004 (to YN) and grants from the Takeda Science Foundation (to SO) and the Mitsubishi Foundation (to YN).

REFERENCES

- Kasai H, Hayami H, Yamaizumi Z, Saitō H, Nishimura S. Detection and identification of mutagens and carcinogens as their adducts with guanosine derivatives. *Nucleic Acids Res* 1984; **12**: 2127–2136.
- Maki H. Origins of spontaneous mutations: specificity and directionality of base-substitution, frameshift, and sequence-substitution mutageneses. *Annu Rev Genet* 2002; **36**: 279–303.
- Boiteux S, Radicella JP. The human OGG1 gene: structure, functions, and its implication in the process of carcinogenesis. *Arch Biochem Biophys* 2000; **377**: 1–8.

- 4 Nakabeppu Y, Kajitani K, Sakamoto K, Yamaguchi H, Tsuchimoto D. MTH1, an oxidized purine nucleoside triphosphatase, prevents the cytotoxicity and neurotoxicity of oxidized purine nucleotides. *DNA Repair* 2006; **5**: 761–772.
- 5 Slupska MM, Baikov C, Luther WM, Chiang JH, Wei YF, Miller JH. Cloning and sequencing a human homolog (*hMYH*) of the *Escherichia coli mutY* gene whose function is required for the repair of oxidative DNA damage. *J Bacteriol* 1996; **178**: 3885–3892.
- 6 Sakamoto K, Tominaga Y, Yamauchi K, Nakatsu Y, Sakumi K, Yoshiyama K et al. MUTYH-null mice are susceptible to spontaneous and oxidative stress induced intestinal tumorigenesis. *Cancer Res* 2007; **67**: 6599–6604.
- 7 Nakabeppu Y, Sakumi K, Sakamoto K, Tsuchimoto D, Tsuzuki T, Nakatsu Y. Mutagenesis and carcinogenesis caused by the oxidation of nucleic acids. *Biol Chem* 2006; **387**: 373–379.
- 8 Takao M, Aburatani H, Kobayashi K, Yasui A. Mitochondrial targeting of human DNA glycosylases for repair of oxidative DNA damage. *Nucleic Acids Res* 1998; **26**: 2917–2922.
- 9 Oka S, Nakabeppu Y. DNA glycosylase encoded by MUTYH functions as a molecular switch for programmed cell death under oxidative stress to suppress tumorigenesis. *Cancer Sci* 2011; **102**: 677–682.
- 10 Takao M, Zhang QM, Yonei S, Yasui A. Differential subcellular localization of human MutY homolog (*hMYH*) and the functional activity of adenine: 8-oxoguanine DNA glycosylase. *Nucleic Acids Res* 1999; **27**: 3638–3644.
- 11 Out AA, Tops CM, Nielsen M, Weiss MM, van Minderhout IJ, Fokkema IF et al. Leiden open variation database of the *MUTYH* gene. *Hum Mutat* 2010; **31**: 1205–1215.
- 12 Sieber OM, Lipton L, Crabtree M, Heinimann K, Fidalgo P, Phillips RK et al. Multiple colorectal adenomas, classic adenomatous polyposis, and germ-line mutations in *MYH*. *New Engl J Med* 2003; **348**: 791–799.
- 13 Al-Tassan N, Chmiel NH, Maynard J, Fleming N, Livingston AL, Williams GT et al. Inherited variants of *MYH* associated with somatic G:C→4T:A mutations in colorectal tumors. *Nat Genet* 2002; **30**: 227–232.
- 14 Oka S, Ohno M, Tsuchimoto D, Sakumi K, Furuichi M, Nakabeppu Y. Two distinct pathways of cell death triggered by oxidative damage to nuclear and mitochondrial DNAs. *EMBO J* 2008; **27**: 421–432.
- 15 Nigro JM, Baker SJ, Preisinger AC, Jessup JM, Hostetter R, Cleary K et al. Mutations in the *p53* gene occur in diverse human tumour types. *Nature* 1989; **342**: 705–708.
- 16 Baker SJ, Preisinger AC, Jessup JM, Paraskeva C, Markowitz S, Willson JK et al. *p53* gene mutations occur in combination with 17p allelic deletions as late events in colorectal tumorigenesis. *Cancer Res* 1990; **50**: 7717–7722.
- 17 Chatterjee A, Mambo E, Osada M, Upadhyay S, Sidransky D. The effect of *p53*-RNAi and *p53* knockout on human 8-oxoguanine DNA glycosylase (*hOgg1*) activity. *FASEB J* 2006; **20**: 112–114.
- 18 Hawn MT, Umar A, Carethers JM, Marra G, Kunkel TA, Boland CR et al. Evidence for a connection between the mismatch repair system and the G2 cell cycle checkpoint. *Cancer Res* 1995; **55**: 3721–3725.
- 19 Papadopoulos N, Nicolaides NC, Wei YF, Ruben SM, Carter KC, Rosen CA et al. Mutation of a *mutL* homolog in hereditary colon cancer. *Science* 1994; **263**: 1625–1629.
- 20 Bronner CE, Baker SM, Morrison PT, Warren G, Smith LG, Lescoe MK et al. Mutation in the DNA mismatch repair gene homologue *hMLH1* is associated with hereditary non-polyposis colon cancer. *Nature* 1994; **368**: 258–261.
- 21 Mitsudomi T, Steinberg SM, Nau MM, Carbone D, D'Amico D, Bodner S et al. *p53* gene mutations in non-small-cell lung cancer cell lines and their correlation with the presence of *ras* mutations and clinical features. *Oncogene* 1992; **7**: 171–180.
- 22 Koi M, Umar A, Chauhan DP, Cherian SP, Carethers JM, Kunkel TA et al. Human chromosome 3 corrects mismatch repair deficiency and microsatellite instability and reduces N-methyl-N'-nitro-N-nitrosoguanidine tolerance in colon tumor cells with homozygous *hMLH1* mutation. *Cancer Res* 1994; **54**: 4308–4312.
- 23 Luo Y, Lin FT, Lin WC. ATM-mediated stabilization of *hMutL*. DNA mismatch repair proteins augments *p53* activation during DNA damage. *Mol Cell Biol* 2004; **24**: 6430–6444.
- 24 Ohtsubo T, Nishioka K, Imaiso Y, Iwai S, Shimokawa H, Oda H et al. Identification of human MutY homolog (*hMYH*) as a repair enzyme for 2-hydroxyadenine in DNA and detection of multiple forms of *hMYH* located in nuclei and mitochondria. *Nucleic Acids Res* 2000; **28**: 1355–1364.
- 25 May E, Jenkins JR, May P. Endogenous HeLa *p53* proteins are easily detected in HeLa cells transfected with mouse deletion mutant *p53* gene. *Oncogene* 1991; **6**: 1363–1365.
- 26 Rodrigues NR, Rowan A, Smith ME, Kerr IB, Bodmer WF, Gannon JV et al. *p53* mutations in colorectal cancer. *Proc Natl Acad Sci USA* 1990; **87**: 7555–7559.
- 27 Riley T, Sontag E, Chen P, Levine A. Transcriptional control of human *p53*-regulated genes. *Nat Rev Mol Cell Biol* 2008; **9**: 402–412.
- 28 Yanamadala S, Ljungman M. Potential role of MLH1 in the induction of *p53* and apoptosis by blocking transcription on damaged DNA templates. *Mol Cancer Res* 2003; **1**: 747–754.
- 29 Kawanishi S, Murata M. Mechanism of DNA damage induced by bromate differs from general types of oxidative stress. *Toxicology* 2006; **221**: 172–178.
- 30 Zhou J, Ahn J, Wilson SH, Prives C. A role for *p53* in base excision repair. *EMBO J* 2001; **20**: 914–923.
- 31 Zaika E, Wei J, Yin D, Andl C, Moll U, El-Rifai W et al. *p73* protein regulates DNA damage repair. *FASEB J* 2011; **25**: 4406–4414.
- 32 de Murcia G, Menissier de Murcia J. Poly(ADP-ribose) polymerase: a molecular nick-sensor. *Trends Biochem Sci* 1994; **19**: 172–176.
- 33 Yu SW, Wang H, Poitras MF, Coombs C, Bowers WJ, Federoff HJ et al. Mediation of poly(ADP-ribose) polymerase-1-dependent cell death by apoptosis-inducing factor. *Science* 2002; **297**: 259–263.
- 34 Galluzzi L, Joza N, Tasdemir E, Mairuri MC, Hengartner M, Abrams JM et al. No death without life: vital functions of apoptotic effectors. *Cell Death Differ* 2008; **15**: 1113–1123.
- 35 Bai H, Jones S, Guan X, Wilson TM, Sampson JR, Cheadle JP et al. Functional characterization of two human MutY homolog (*hMYH*) missense mutations (R227W and V232F) that lie within the putative hMSH6 binding domain and are associated with *hMYH* polyposis. *Nucleic Acids Res* 2005; **33**: 597–604.
- 36 Gu Y, Parker A, Wilson TM, Bai H, Chang DY, Lu AL. Human MutY homolog, a DNA glycosylase involved in base excision repair, physically and functionally interacts with mismatch repair proteins human MutS homolog 2/human MutS homolog 6. *J Biol Chem* 2002; **277**: 11135–11142.
- 37 Kanagaraj R, Parasuraman P, Mihaljevic B, van Loon B, Burdova K, Konig C et al. Involvement of Werner syndrome protein in MUTYH-mediated repair of oxidative DNA damage. *Nucleic Acids Res* 2012; **40**: 8449–8459.
- 38 Haugen AC, Goel A, Yamada K, Marra G, Nguyen TP, Nagasaka T et al. Genetic instability caused by loss of MutS homologue 3 in human colorectal cancer. *Cancer Res* 2008; **68**: 8465–8472.
- 39 Tseng-Rogenski SS, Chung H, Wilk MB, Zhang S, Iwaizumi M, Carethers JM. Oxidative stress induces nuclear-to-cytosol shift of hMSH3, a potential mechanism for EMAT in colorectal cancer cells. *PLoS ONE* 2012; **7**: e50616.
- 40 Stambolsky P, Weisz L, Shats I, Klein Y, Goldfinger N, Oren M et al. Regulation of AIF expression by *p53*. *Cell Death Differ* 2006; **13**: 2140–2149.
- 41 Godefroy N, Lemaire C, Renaud F, Rincheval V, Perez S, Parvu-Ferecatu I et al. *p53* can promote mitochondria- and caspase-independent apoptosis. *Cell Death Differ* 2004; **11**: 785–787.
- 42 Ren SX, Cheng AS, To KF, Tong JH, Li MS, Shen J et al. Host immune defense peptide LL-37 activates caspase-independent apoptosis and suppresses colon cancer. *Cancer Res* 2012; **72**: 6512–6523.
- 43 Johnson MD, Kinoshita Y, Xiang H, Ghatan S, Morrison RS. Contribution of *p53*-dependent caspase activation to neuronal cell death declines with neuronal maturation. *J Neurosci* 1999; **19**: 2996–3006.
- 44 Hooper C, Meimariou E, Tavassoli M, Melino G, Lovestone S, Killick R. *p53* is upregulated in Alzheimer's disease and induces tau phosphorylation in HEK293a cells. *Neurosci Lett* 2007; **418**: 34–37.
- 45 Ohyagi Y, Asahara H, Chui DH, Tsuruta Y, Sakae N, Miyoshi K et al. Intracellular Aβ42 activates *p53* promoter: a pathway to neurodegeneration in Alzheimer's disease. *FASEB J* 2005; **19**: 255–257.
- 46 Shimura-Miura H, Hattori N, Kang D, Miyako K, Nakabeppu Y, Mizuno Y. Increased 8-oxo-dGTPase in the mitochondria of substantia nigral neurons in Parkinson's disease. *Ann Neurol* 1999; **46**: 920–924.
- 47 Sheng Z, Oka S, Tsuchimoto D, Abolhassani N, Nomaru H, Sakumi K et al. 8-Oxoguanine causes neurodegeneration during MUTYH-mediated DNA base excision repair. *J Clin Invest* 2012; **122**: 4344–4361.
- 48 Arai T, Fukae J, Hatano T, Kubo S, Ohtsubo T, Nakabeppu Y et al. Up-regulation of *hMUTYH*, a DNA repair enzyme, in the mitochondria of substantia nigra in Parkinson's disease. *Acta Neuropathol* 2006; **112**: 139–145.
- 49 Scheffner M, Takahashi T, Huibregtse JM, Minna JD, Howley PM. Interaction of the human papillomavirus type 16 E6 oncoprotein with wild-type and mutant human *p53* proteins. *J Virol* 1992; **66**: 5100–5105.
- 50 Nishioka K, Ohtsubo T, Oda H, Fujiwara T, Kang D, Sugimachi K et al. Expression and differential intracellular localization of two major forms of human 8-oxoguanine DNA glycosylase encoded by alternatively spliced OGG1 mRNAs. *Mol Biol Cell* 1999; **10**: 1637–1652.



Oncogenesis is an open-access journal published by Nature Publishing Group. This work is licensed under a Creative Commons Attribution-NonCommercial-NoDerivs 4.0 International License. The images or other third party material in this article are included in the article's Creative Commons license, unless indicated otherwise in the credit line; if the material is not included under the Creative Commons license, users will need to obtain permission from the license holder to reproduce the material. To view a copy of this license, visit <http://creativecommons.org/licenses/by-nc-nd/4.0/>